

Stochastic mean-shift clustering

Itshak Lapidot^{a,b}, Yann Sepulcre^c, Tom Trigano^d

^a*Afeka Tel-Aviv Academic College of Engineering, School of Electrical Engineering, Israel*

^b*Avignon University, LIA, France*

^c*Sapir Academic College, Department of Engineering, Sderot, Israel*

^d*Shamoon College of Engineering, Department of Electrical Engineering, Ashdod, Israel*

Abstract

We present a stochastic version of the mean-shift clustering algorithm. In this stochastic version a randomly chosen sequence of data points move according to partial gradient ascent steps of the objective function. Theoretical results illustrating the convergence of the proposed approach, and its relative performances is evaluated on synthesized 2-dimensional samples generated by a Gaussian mixture distribution and compared with state-of-the-art methods. It can be observed that in most cases the stochastic mean-shift clustering outperforms the standard mean-shift. We also illustrate as a practical application the use of the presented method for speaker clustering.

Keywords:

Unsupervised learning, Mean-shift clustering, Stochastic mean-shift, non-parametric PDF estimation.

Email addresses: itshakl@afeka.ac.il (Itshak Lapidot),
yanns@mail.sapir.ac.il (Yann Sepulcre), thomast@sce.ac.il (Tom Trigano)

1. Introduction

Clustering algorithms are still actively investigated due to their many areas of application. Numerous algorithms have been proposed and investigated, among which the k -means [1], Spectral clustering [2, 3], DBSCAN [4], and the well-known *Mean-shift* (MS) clustering algorithm. MS is an effective non-parametric iterative algorithm [5], which is versatile for clustering, tracking, and smoothing tasks. A well-known and used variant of MS is the *blurring mean-shift* (BMS) [6]. Both MS and BMS algorithms can be coined “deterministic” iterative procedures aiming to find local maximizers of an objective function, since they do not involve any random selection of points to perform their update rule.

Both MS and BMS algorithms have been applied to a variety of domains, and several variations around their original formulation have been proposed: see [7] for BMS with a Gaussian kernel (known as Gaussian blurring mean-shift); for BMS applied to high-dimensional data clustering see [8]. Applications in image processing include image segmentation [9], medical and satellite images feature extraction [10, 11] and videos segmentation [12]. In speech processing, an adaptive version of MS has been used to segment speaker clusters [13, 14, 15, 16]. The mathematical properties of the convergence of these algorithms have also been thoroughly investigated: [17, 18] investigated convergence properties, while [19] provided a unifying view for density-based clustering and clarifies mean-shift-style mode-seeking mechanics for image analysis.

With the growing size of modern datasets and increasing resolution of data collected by instruments, there is a real need to improve existing algo-

rithms. One possible direction is to enhance its convergence rate. Regarding the MS for instance, a version involving randomly chosen subsets of points has been proposed in [20], which is known to be suboptimal; in settings with a large number of data points but low dimensionality, the MeanShift++ (or Extremely Fast Mode-Seeking) proposed in [21] is significantly faster than MS with similar performances; subsequent improvement of this method, particularly suitable for high dimensionality datasets can be found in [22]. Another direction for MS improvement is to obtain a better convergence with more significant clusters. [23] suggested a robust version of MS, which leads to fewer outlier clusters and faster convergence. [24] proposed a Mean-Shift Outlier Detector that uses mean-shift density/location updates to reduce bias from outliers and to filter less relevant data points, while [25] adapted mean-shift ideas to a granular-ball (coarse-to-fine) representation to improve outlier detection and computational behavior. To address specific structure clustering, [26] extended the BMS to a version that could be applied to data lying on a manifold.

In this work we present a stochastic variant of BMS called *Stochastic Mean Shift* (SMS), where the data sample points (defining the current state) move one after the other along a climbing path of an objective function, one single point being randomly chosen and moved to a different location at each step; it can still be considered to be a blurring process since the updated points are never replaced to their original locations and keep moving from their current position; at each step any sample point can be picked up for update. The paper also presents theoretical results on its convergence.

Random, asynchronous updates in SMS are preferred for two main rea-

sons. First, updating points one at a time improves convergence stability by preventing the ordinary mean shift from converging to "false modes" that arise when neighboring points use outdated information in noisy or high-dimensional settings. Second, these asynchronous updates allow for in-place computation, which reduces memory usage—a crucial benefit when working with large datasets.

The paper is organized as follows. Section 2 presents the main competing clustering algorithms, including the SMS . We then introduce the theoretical results on SMS , and discuss its convergence. We present in section 4 clustering evaluation criteria used for evaluation, and detail results obtained for these clustering algorithms on synthetic datasets. As an application, we also illustrate the application of SMS on speaker clustering tasks in section 5. Proofs of the presented results are detailed in the supplementary material.

2. Description of the Stochastic Mean Shift (SMS)

The following section presents our stochastic version of MS . For comparison, we first recall the Mean-shift (MS) and the Blurring mean-shift (BMS). Table 1 summarizes the notations used in this paper.

First, we provide details on the specific kernels to be considered in this work. These assumptions will be further used in the theoretical proofs.

- Definition 1.**
1. We call a profile function a mapping $k : [0, 1] \rightarrow \mathbb{R}_+$ that is C^1 , non-increasing, convex and such that $k'(t) < 0$ for all $t \in [0, 1)$.
 2. a multivariate function which can be written as $K(\mathbf{u}) = k(\|\mathbf{u}\|^2)$ for all $\mathbf{u} \in \mathbb{R}^d$ will be referred to as a kernel with profile function k .

Table 1: Summary of the main notations used throughout the paper

Notation	Significance
General notations	
$[n]$	the set of integers $\{1, \dots, n\}$
\mathbb{R}_+	the set of non negative reals $[0, \infty)$
2^S	the collection of all subsets of a set S
$\ \mathbf{u}\ , \mathbf{u} \in \mathbb{R}^{n \times 1}$	the ℓ_2 norm of \mathbf{u}
Specific notations	
x_1, \dots, x_J	The J data points
$K(\mathbf{u}) = k(\ \mathbf{u}\ ^2); G(\mathbf{u}) = -k'(\ \mathbf{u}\ ^2)$	density kernel K on \mathbb{R}^n associated to the profile $k : [0, \infty) \rightarrow \mathbb{R}_+$; "weight" function on \mathbb{R}^n
$N_h(x), x \in \mathbb{R}^d$	subset of $[n]$ of the neighboring indices $\{i : \ x - \mathbf{x}_i\ < h\}$
i_k	the index $i \in [n]$ randomly chosen at the k^{th} step of SMS
$\nabla_i L$	partial gradient $\nabla_{\mathbf{x}_i} L$ of L w.r.t the variable \mathbf{x}_i
$\nabla^{(k)}; \nabla_i^{(k)}$	gradient of L at step k of SMS ; partial gradient $\nabla_i L$ at step k of SMS
$\ \mathbf{U}\ , \mathbf{U} = [\mathbf{u}_1^T, \dots, \mathbf{u}_n^T]^T, \mathbf{u}_i \in \mathbb{R}^{d \times 1}$	$\max_{i \in [n]} \ \mathbf{u}_i\ _2$: maximal component wise ℓ_2 norm value

Typical examples of such profiles and associated kernels include $k(t) = (1 - t)_+^\alpha$ for $\alpha = 2, 3, 4$, which lead respectively to the Bi-, Tri-, and Quad-weights kernels $K(\mathbf{u}) = (1 - \|\mathbf{u}\|^2)_+^\alpha$, respectively.

For any sample set $\{\mathbf{x}_i\}_{i \in [n]}$ with $\mathbf{x}_i \in \mathbb{R}^d, i = 1 \dots n$, stemming from some unknown multi-modal density f_X defined on \mathbb{R}^d , given a kernel K and a positive bandwidth parameter $h > 0$, the kernel density estimate (KDE) of f_X associated with $\{\mathbf{x}_i\}_{i \in [n]}$ is defined as

$$\forall x \in \mathbb{R}^d \quad D(x) = \frac{1}{nh^d} \sum_{i \in [n]} K\left(\frac{1}{h}(x - \mathbf{x}_i)\right). \quad (1)$$

Since all the considered kernels have compact support by definition of the profile functions, this property is shared by any KDE defined in (1). For the rest of this paper, we shall refer to the element $\mathcal{X} = [\mathbf{x}_1^T, \dots, \mathbf{x}_n^T]^T \in \mathbb{R}^{dn}$ as the *state* defined by this sample, and interpret any iterative clustering algorithm as a chain of transformations of \mathbb{R}^{dn} applied to the initial state

$\mathcal{X}^{(0)}$ given by the raw sample until we reach convergence (in a sense to be precised). A state shall be introduced further shortly as $\mathcal{X} = [\mathbf{x}_i]_{i \in [n]}$ for the sake of simplicity, without emphasizing further the implicit vector structure.

2.1. Reminders on MS and BMS

MS works under the mild assumption that dense regions in the data space correspond to modes of f_X , which can be estimated by the local maxima of (1). All points are updated to the weighted average of neighboring points, where weights are determined by their distance, until convergence around modes of the estimated distribution (1).

Mathematically, MS is a gradient ascent algorithm on D which aims to provide convergence to a local maximizer. This formulation can be found in several references, such as [20] and [27]. For any state \mathcal{X} , we shall consider the *mean-shift operator* $\mathcal{S}_h : \mathbb{R}^d \rightarrow \mathbb{R}^d$ which maps a point $x \in \mathbb{R}^d$ to its new position as

$$\mathcal{S}_h(x; \mathcal{X}) = \frac{\sum_{i \in [n]} G\left(\frac{x - \mathbf{x}_i}{h}\right) \mathbf{x}_i}{\sum_{i \in [n]} G\left(\frac{x - \mathbf{x}_i}{h}\right)}, \quad (2)$$

where $G(\mathbf{u}) = -k'(\|\mathbf{u}\|^2)$ defines the non-negative *weight function* associated with K . Note that the denominator in (2) is always positive since $-k'(0) > 0$. Note also that (2) is effectively computed on the \mathcal{X} -*neighborhood* of x which is defined as

$$N_h(x) = \left\{ i \in [n] \mid G\left(\frac{x - \mathbf{x}_i}{h}\right) \neq 0 \right\} = \{i \in [n] \mid \|x - \mathbf{x}_i\| < h\},$$

since K has a radial symmetry. The *shift vector* of x is defined as

$$\mathbf{m}_h(x; \mathcal{X}) = \mathcal{S}_h(x; \mathcal{X}) - x \quad ; \quad (3)$$

it can be easily verified that $\mathbf{m}_h(x)$ is indeed proportional to the gradient of D taken at x , thus allowing to consider MS as a gradient ascent method on D with variable step-size. As a particular case, when using the Epanechnikov kernel, the shift vector $m_h(x)$ is defined as follows:

$$m_h(x) = \frac{\sum_{i \in N_h(x)} \mathbf{x}_i}{\#N_h(x)} - x \quad (4)$$

where $\#$ denotes the cardinality of the set $N_h(x)$. Details on its convergence can be found in [28].

The Blurring mean-shift (BMS) is a related kernel-based iterative method for data clustering, which aims to improve MS. Starting from the initial state $\mathcal{X}^{(0)} \in \mathbb{R}^{dn}$ defined by the original data sample, for any $k \in \mathbb{N}_0$ the k^{th} step of the BMS consists in updating the current state $\mathcal{X}^{(k)}$ to the new state $\mathcal{X}^{(k+1)}$ by applying the mean-shift operator defined as follows:

$$\forall i \in [n] \quad \mathbf{x}_i^{(k+1)} = \frac{\sum_{j=1}^n G\left(\frac{\mathbf{x}_i^{(k)} - \mathbf{x}_j^{(k)}}{h}\right) \mathbf{x}_j^{(k)}}{\sum_{j=1}^n G\left(\frac{\mathbf{x}_i^{(k)} - \mathbf{x}_j^{(k)}}{h}\right)} \quad (5)$$

In other words, we apply to each sample point the mean-shift operator to find its new location, but by plugging in (2) the current state $\mathcal{X}^{(k)}$. Hence, in contrast with MS, the points move altogether during the whole process, as summarized in Algorithm 1b.

From a mathematical point of view, the BMS algorithm can be seen as an iterative procedure aimed at converging to a local maximizer of the following non-negative objective function

$$\forall \mathcal{X} = [\mathbf{x}_1^T, \dots, \mathbf{x}_n^T]^T \in \mathbb{R}^{dn} \quad L(\mathcal{X}) = \sum_{1 \leq i < j \leq n} K\left(\frac{1}{h}(\mathbf{x}_i - \mathbf{x}_j)\right) \quad ; \quad (6)$$

Indeed one can reformulate (5) as a "weighted" gradient step as follows:

$$\mathcal{X}^{(k+1)} = \mathcal{X}^{(k)} + \frac{h^2}{2} \sum_{i=1}^n \frac{1}{\sum_{j=1}^n G\left(\frac{\mathbf{x}_i^{(k)} - \mathbf{x}_j^{(k)}}{h}\right)} \nabla_{\mathbf{x}_i} L(\mathcal{X}^{(k)}) \quad (7)$$

where $\nabla_{\mathbf{x}_i} L(\mathcal{X})$ denotes the gradient component of L related to the \mathbf{x}_i direction. Any state $\mathcal{X} \in \mathbb{R}^{dn}$ satisfies $\nabla L(\mathcal{X}) = \mathbf{0}_{dn}$ if and only if it is a fixed point of the transformation (5), i.e.

$$\forall i \in [n] \quad \mathbf{x}_i = \frac{\sum_{j=1}^n G\left(\frac{\mathbf{x}_i - \mathbf{x}_j}{h}\right) \mathbf{x}_j}{\sum_{j=1}^n G\left(\frac{\mathbf{x}_i - \mathbf{x}_j}{h}\right)} \quad (8)$$

The relation between the stationary points of L and our clustering objective is made explicit in a theorem from [18], which can be written as follows:

Theorem 1. *Assume the profile function k of the kernel K satisfies assumptions a) – c). A state $\mathcal{X} = [\mathbf{x}_1^T, \dots, \mathbf{x}_n^T]^T \in \mathbb{R}^{dn}$ satisfies $\nabla L(\mathcal{X}) = \mathbf{0}_{dn}$ iff the following is satisfied:*

$$\forall (i, j) \in [n]^2 \quad j \in N_h(\mathbf{x}_i) \iff \mathbf{x}_j = \mathbf{x}_i \quad (9)$$

In other words, for the specific truncated kernels considered in this study, a critical point of L is a state satisfying an ideal clustering condition: two points either coincide, or are distant from h at least. In the previous theorem, (9) will be later used to prove theoretical results on the effectiveness of the stochastic mean-shift, which is introduced in the next subsection.

Convergence of the BMS sequence has been thoroughly investigated and proved [17]; theorems establishing convergence rates for different kernel types

can be found in [18]. Though BMS may converge faster than MS , its algorithmic complexity is roughly $O(n^2)$, which makes it computationally expensive for large datasets.

2.2. Stochastic mean-shift algorithm

We now present the *stochastic mean-shift* algorithm (SMS), which is the main novelty of this paper. Roughly speaking, SMS can be seen as a trade-off between MS and BMS , adding some randomness in the shifting process. Its principle is as follows: starting from an original state $\mathcal{X}^{(0)} = [\mathbf{x}_j]_{j=1}^n$, in each subsequent step k an index $i \in [n]$ is picked up randomly (according to the uniform distribution and independently of all previous choices), and the chosen point alone is moved by using the shift operator \mathcal{S}_h , by plugging in (2) the sample $[\mathbf{x}_j^{(k)}]$ considered in its *current state*. In other words, and similarly to BMS , all the sample points may move during the whole process. A summarized version of SMS is described in Algorithm 1c.

SMS can be interpreted as some "partial" gradient algorithm: starting from some initial state $\mathcal{X}^{(0)} \in \mathbb{R}^{nd}$, the k^{th} step of SMS consists in picking randomly an index $i_k \in \{1, \dots, n\}$ and defining the $k + 1$ state as

$$\mathcal{X}^{(k+1)} = \mathcal{X}^{(k)} + \frac{h^2/2}{\sum_{j=1}^n G\left(\frac{\mathbf{x}_{i_k}^{(k)} - \mathbf{x}_j^{(k)}}{h}\right)} \nabla_{\mathbf{x}_{i_k}} L(\mathcal{X}^{(k)}) \quad (10)$$

where $\nabla_{\mathbf{x}_i} L(\mathcal{X})$ denotes the partial gradient of L in the \mathbf{x}_i direction. It follows immediately that algorithm 1c has a linear complexity $O(k)$, k denoting the overall number of draws.

<pre> for $\mathbf{x}_i \in \mathcal{X}$ do while Convergence is not attained do $\mathbf{x}_i^{(k+1)} \leftarrow \mathcal{S}_h(\mathbf{x}_i^{(k)}; \mathcal{X})$ $k + 1 \leftarrow k$ Convergence diagnosis end while end for </pre> <p style="text-align: center;">(a) Mean-Shift</p>	<pre> while Convergence is not attained do for $\mathbf{x}_i^{(k)} \in \mathcal{X}^{(k)}$ do $\mathbf{x}_i^{(k+1)} \leftarrow \mathcal{S}_h(\mathbf{x}_i^{(k)}; \mathcal{X}^{(k)})$ end for $k + 1 \leftarrow k$ Convergence diagnosis end while </pre> <p style="text-align: center;">(b) Blurring Mean-Shift</p>	<pre> while Convergence is not at- tained do Draw the index $I_k \in [n]$ uniformly $\mathbf{x}_{I_k}^{(k+1)} \leftarrow \mathcal{S}_h(\mathbf{x}_{I_k}^{(k)}; \mathcal{X}^{(k)})$ $k + 1 \leftarrow k$ Convergence diagnosis end while </pre> <p style="text-align: center;">(c) Stochastic Mean-Shift</p>
--	---	---

Algorithms 1: Comparison between Mean-Shift, Blurring Mean-Shift and Stochastic Mean-Shift. In all cases, convergence diagnosis is either based on a maximal number of iterations or when $\|\mathbf{x}_i^{(k+1)} - \mathbf{x}_i^{(k)}\|$ is smaller than a user-defined threshold

3. Theoretical results

We now show that for an SMS sequence, the points partition into clusters becomes fixed almost surely after a finite number of steps provided one use an appropriate distance threshold to assess similarity (see theorem 2). We also establish in theorem 3 that under the restrictive assumption that the distances between any two points in $\mathcal{X}^{(0)}$ are less than h , the sample points converge almost surely to the same limit point as k tends to infinity. Though we could not establish in general an a.s. convergence of $\mathcal{X}^{(k)}$, our primary purpose in this work remains effective data clustering, which is indeed achieved by SMS .

Unless stated otherwise, in this section we suppose given any kernel K defined on \mathbb{R}^d , associated to a profile k satisfying all of the assumptions a)–c) exposed in the beginning of section 2; all notations, definitions, and assumptions introduced there will be used in the present section. The presented

results' proofs are postponed to the supplementary material.

3.1. Ascending property of Stochastic Mean Shift

We consider a state $\mathcal{X} \in \mathbb{R}^{nd}$, i.e. an ordered set of n points $\mathcal{X} = [\mathbf{x}_1^T, \dots, \mathbf{x}_n^T]^T$ such that $\mathbf{x}_i \in \mathbb{R}^d$ for each i ; given also some positive parameter $h > 0$, we already saw that SMS can be interpreted as some partial gradient steps process applied to the function $L(\mathcal{X}) = \sum_{1 \leq i \leq j \leq n} K\left(\frac{1}{h}(\mathbf{x}_i - \mathbf{x}_j)\right)$; clearly L is non negative, C^1 and bounded from above by the absolute maximal value $\frac{n(n+1)}{2}k(0)$ which is attained in states such that $\mathbf{x}_i = \mathbf{x}_j$ for any $1 \leq i, j \leq n$; there are infinitely many critical points of L (in the sense that $\nabla L(\mathcal{X}) = \mathbf{0}_{dn}$) since L is invariant through any isometry of \mathbb{R}^d applied component-wise to \mathcal{X} (these are the states satisfying (8) as previously mentioned). Starting from some initial state $\mathcal{X}^{(0)} \in \mathbb{R}^{nd}$, the k^{th} step of SMS consists in picking randomly an index $i_k \in \{1, \dots, n\}$ and defining the $k + 1$ state as

$$\mathcal{X}^{(k+1)} = \mathcal{X}^{(k)} + \frac{h^2/2}{\sum_{j=1}^n G\left(\frac{\mathbf{x}_{i_k}^{(k)} - \mathbf{x}_j^{(k)}}{h}\right)} \nabla_{\mathbf{x}_{i_k}} L(\mathcal{X}^{(k)}), \quad (11)$$

where $\nabla_{\mathbf{x}_i} L(\mathcal{X})$ denotes the gradient of L in the \mathbf{x}_i direction. Since the initial state $\mathcal{X}^{(0)}$ is given, at any step $k \geq 1$ of SMS the state $\mathcal{X}^{(k)}$ depends solely on the random sequence of indices $[i_{k-1}, \dots, i_0]$, i.e. there exists a non-random function $F^{(k)} : [n]^k \rightarrow \mathbb{R}^{dn}$ such that $\mathcal{X}^{(k)} = F^{(k)}[i_{k-1}, \dots, i_0]$.

In the following, we shall denote the partial gradient $\nabla_{\mathbf{x}_i} L$ w.r.t. the variable \mathbf{x}_i by $\nabla_i L$ for simplicity.

The following preliminary result shows that the value of L is non-decreasing at any step (11) of SMS .

Proposition 1. *Given any initial state $\mathcal{X}^{(0)} \in \mathbb{R}^{dn}$, for any $k \in \mathbb{N}$ it holds that*

$$L(\mathcal{X}^{(k+1)}) - L(\mathcal{X}^{(k)}) \geq C \|\mathbf{x}_{i_k}^{(k+1)} - \mathbf{x}_{i_k}^{(k)}\|^2 \quad (12)$$

for some constant $C > 0$, with $i_k \in [n]$ denoting the randomly chosen index at step k . Two consequences follow from (12):

- 1) the sequence $(L(\mathcal{X}^{(k)}))_{k \in \mathbb{N}}$ of the L values of the SMS states is non decreasing and convergent ;
- 2) it holds furthermore that for a positive constant D (depending only on n, h and the kernel K):

$$\|\nabla_{i_k} L(\mathcal{X}^{(k)})\| \leq D \sqrt{L(\mathcal{X}^{(k+1)}) - L(\mathcal{X}^{(k)})} ; \quad (13)$$

hence $\nabla_{i_k} L(\mathcal{X}^{(k)}) \rightarrow \mathbf{0}_d$ a.s as $k \rightarrow \infty$.

Remark 1. *An easy consequence of (13) is that for any $\epsilon > 0$, it holds a.s that*

$$\#\{j \mid \|\nabla_{i_j} L(\mathcal{X}^{(j)})\| \geq \epsilon\} \leq \left(\frac{D}{\epsilon}\right)^2 \left[\frac{n(n+1)}{2}k(0) - L(\mathcal{X}^{(0)})\right]$$

3.2. Clustering and convergence results for SMS

Proposition 1 showed that in the SMS algorithm, the sequence of partial gradients of L (computed at each step w.r.t. the randomly selected variable) tends to 0 a.s. Since for each $k \in \mathbb{N}$ the index i_k is drawn from the uniform distribution on $[n]$ and independently of the sequence $[i_{k-1}, \dots, i_1]$, we will show at proposition 2 that the whole gradient $\nabla L(\mathcal{X}^{(k)}) \rightarrow \mathbf{0}$ a.s.

We first introduce sequences of stopping times, which shall be used in the proofs. In all of the sequel we use the following notations: at step $k \in \mathbb{N}$ of the SMS algorithm, the gradient $\nabla L(\mathcal{X}^{(k)})$ shall be denoted by $\nabla^{(k)}$; hence $\nabla_i^{(k)}$ shall denote $\nabla_{\mathbf{x}_i} L(\mathcal{X}^{(k)})$ for any $i \in [n]$; and $\|\nabla^{(k)}\|$ shall denote the norm $\max_{i \in [n]} \|\nabla_i^{(k)}\|_2$ i.e the maximal component wise ℓ_2 norm value of the gradient $\nabla^{(k)}$.

Suppose given now any $\epsilon > 0$ and any fixed positive integer k_0 ; for any $t > k_0$ we define the following event $A_t = \left\{ \forall k \in (k_0, \dots, t] \|\nabla_{i_k}^{(k)}\| < \epsilon \right\}$; in other words A_t occurs if and only if for each $k_0 < k \leq t$ the partial gradient computed w.r.t the selected variable \mathbf{x}_{i_k} has a norm smaller than ϵ . We define a first stopping time as

$$T_1 = \min \{t > k_0 \mid \|\nabla^{(t)}\| \geq \epsilon \wedge A_t\} ; \quad (14)$$

in case there is no $t > k_0$ satisfying the condition above, then we set $T_1 = \infty$. We further define for any integer $p \geq 2$ a p^{th} stopping time T_p by the following recursive way:

$$T_p = \min \{t > T_{p-1} \mid \|\nabla^{(t)}\| \geq \epsilon \wedge A_t\} , \quad (15)$$

setting $T_p = \infty$ in case $T_{p-1} = \infty$ or if there is no $t > T_{p-1}$ satisfying the condition. Note that the sequence $(T_p)_{p \in \mathbb{N}}$ is indeed a sequence of stopping times w.r.t the SMS indices sequence $[i_k]_{k \in \mathbb{N}}$ since for any $p \in \mathbb{N}$ and $k \in \mathbb{N}$ it holds that $(T_p = k) \in \sigma \{i_j ; j \in [k]\}$.

Lemma 1. *Given any positive real $\epsilon > 0$ and fixed positive integer k_0 as before, define the sequence (T_p) of stopping times as in (14)(15); for any $p \in \mathbb{N}$ we define the event $\Omega_p = \{T_p < \infty\}$. The following conclusion holds: $\mathbb{P}(\Omega_p) \leq \left(1 - \frac{1}{n}\right)^p$, hence $\lim_{p \rightarrow \infty} \mathbb{P}(\Omega_p) = 0$.*

Lemma 1 yields the following proposition.

Proposition 2. *Given any initial state $\mathcal{X}^{(0)} \in \mathbb{R}^{dn}$, the SMS sequence satisfies $\nabla^{(k)} \rightarrow \mathbf{0}_{dn}$ holds a.s as $k \rightarrow \infty$.*

The main clustering result is now presented. It states that almost surely, after a specific step in the SMS, well-separated and stable clusters are observed.

Theorem 2. *Given any state $\mathcal{X}^{(0)} \in \mathbb{R}^{dn}$, let $(\mathcal{X}^{(k)})$ be the SMS states sequence; suppose τ is any given real in $(0, \frac{h}{2})$. Then there exists a.s some partition J_1, \dots, J_M of $[n]$ and $K \in \mathbb{N}$ such that for every $k \geq K$:*

$$1) \text{ for any } l \in [M] \text{ it holds that } \max_{\substack{i \in J_l \\ j \in J_l}} \|\mathbf{x}_i^{(k)} - \mathbf{x}_j^{(k)}\| < \tau \quad ;$$

$$2) \text{ for any } (l, m) \in [M]^2 \text{ s.t } l \neq m, \text{ it holds that } \min_{\substack{i \in J_l \\ j \in J_m}} \|\mathbf{x}_i^{(k)} - \mathbf{x}_j^{(k)}\| > h - \tau \quad ;$$

in other words a.s. the points $\mathbf{x}_1^{(k)}, \dots, \mathbf{x}_n^{(k)}$ belong to fixed clusters for sufficiently large k , the l^{th} cluster being defined as $\mathcal{C}_l = \{\mathbf{x}_i^{(k)}, i \in J_l\}$ (for all sufficiently large k); moreover all clusters diameters tend a.s to 0 as $k \rightarrow \infty$.

It could be noted that the existence of such fixed clusters does not imply that a.s. the state $\mathcal{X}^{(k)}$ converges in \mathbb{R}^{dn} . Though we could not generally prove that the SMS sequence converges a.s., we establish below a convergence result in the particular case of a sample of diameter less than h (thus yielding a single cluster whichever trajectory the SMS may take). The first part of the proof follows a similar argument from [17].

Theorem 3. *Suppose $(\mathcal{X}^{(k)})_{k \in \mathbb{N}_0}$ is a SMS sequence obtained with a kernel K associated to a profile k satisfying assumptions a) – c). Suppose the initial state $\mathcal{X}^{(0)} \in \mathbb{R}^{dn}$ satisfies that $\forall (i, j) \in [n]^2 \|\mathbf{x}_i^{(0)} - \mathbf{x}_j^{(0)}\| < h$. Then a.s there exists $\mathbf{x} \in \mathbb{R}^d$ such that $\forall i \in [n] \lim_{k \rightarrow \infty} \mathbf{x}_i^{(k)} = \mathbf{x}$.*

3.3. Practical Convergence Diagnosis

Given an initial state $\mathcal{X}^{(0)} \in \mathbb{R}^{dn}$, the minimal number k of SMS steps which are necessary to achieve the aforementioned clustering is by nature a random variable. No theoretical results in this paper provide further precision about a higher bound on k which would hold under a specified high probability. Though each step costs linearly in n since we shift only one point at a time, an SMS process as described in algorithm 1c might need more steps than its BMS or MS counterparts in order to achieve the desired clustering. This constraint makes it necessary to define convenient stopping criteria, even if the clustering above has not been completely achieved yet. In practice, whenever a sufficient number of points have a sufficiently small last shift, the algorithm stops. Such a practice is justified by the conclusions of propositions 1 and 2.

4. Results and Discussion on Synthetic Data

This section presents the results and their discussion for simulated, synthetic data. In synthetic data, we compared the behavior of MS, BMS, and SMS. All the experiments were performed using MATLAB R2025a, on an i9 Intel computer with 32 GB of RAM. Code is made available upon request for reproducibility.

4.1. External evaluation criteria for clustering performance

Though clustering performance can be assessed using intrinsic, task-independent, criteria (see e.g. [29, chapter 17] or [30, 31]), Instead, we shall follow a second common approach, which typically relies on external, task-dependent evaluation criteria. More specifically, clustering results will be compared to predefined labels describing the data. In this framework, a common way to evaluate clustering performance is using a notion of cluster or class purity, which can be expressed in several ways. The general idea is to quantify similarity between two partitions of the data sample, the first induced by the predefined classes and the other induced by the clustering outcome. In this paper, we rely on the notions of the quantity K introduced below in (20), which is itself based on the notions of *average cluster purity (ACP)* and *average label purity (ALP)* defined in [16], and on the quantity G introduced in (17), which itself relies on the notions of cluster purity. We briefly recall their definitions for convenience. Following [29], our first evaluation criteria are introduced below, and rely on the following two quantities:

$$Pur(\mathcal{C}, \mathcal{D}) = \frac{1}{N} \sum_{q=1}^Q \max_{d_r \in \mathcal{D}} n_{qr} \quad ; \quad Pur(\mathcal{D}, \mathcal{C}) = \frac{1}{N} \sum_{r=1}^R \max_{c_q \in \mathcal{C}} n_{qr} \quad (16)$$

where $n_{q,r}$ denotes the total number of data points in cluster c_q associated with the true label d_r , $\mathcal{C} = \{c_q ; 1 \leq q \leq Q\}$ is the set of all the obtained clusters and $\mathcal{D} = \{d_r ; 1 \leq r \leq R\}$ is the set of all true labels. $Pur(\mathcal{C}, \mathcal{D})$ is traditionally defined as the clustering "purity" (w.r.t. the ground truth) and is equal to the optimal success rate that can be achieved by a rule assigning all points of a given cluster to one class. Similarly, $Pur(\mathcal{D}, \mathcal{C})$ defines class purity (w.r.t the clustering). Our first measure of clustering performance

shall be the following trade-off quantity:

$$G = \sqrt{Pur(\mathcal{C}, \mathcal{D}) \cdot Pur(\mathcal{D}, \mathcal{C})} \in (0, 1]. \quad (17)$$

The purpose of the quantities ACP and ALP introduced below is to define how far the probability of belonging to a cluster conditionally on its label and the probability of having a given label conditionally on the belonging cluster differ from Kronecker’s delta distributions, in an average sense, and for uniform priors. More specifically, we define

$$ACP = \frac{1}{Q} \sum_{q=1}^Q \sum_{r=1}^R P(d_r|c_q)^2 \quad (18)$$

$$ALP = \frac{1}{R} \sum_{r=1}^R \sum_{q=1}^Q P(c_q|d_r)^2 \quad (19)$$

where in the latter $P(d_r|c_q)$ the probability for a point of the cluster c_q to have the true label d_r and $P(c_q|d_r)$ the probability for a point with known label d_r to belong to the cluster c_q , respectively. The inner sums in (18) and (19) can also be seen as a purity index of the cluster c_q and a purity index for label d_r , respectively. Roughly speaking, lower values of ACP occur whenever the clusters are not class homogeneous. In contrast, lower values of ALP occur whenever the classes are decomposed along several clusters (both in an average sense). Taking both aspects into account can be done by considering the geometric average, which will also be investigated:

$$K = \sqrt{ACP \cdot ALP} \in (0, 1] \quad (20)$$

4.2. Multi-modal data clustering

We present clustering results for visual inspection and discussion. The synthetic data was generated using a bidimensional Gaussian mixture of three

Table 2: Hyperparameters used in multi-modal clustering experiments

	Set 1	Set 2	Set 3	Set 4
Number of clusters	3			
Gaussian expectations	$m_1 = [1 \ 1]^T, m_2 = [-1 \ -1]^T, m_3 = [1 \ -1]^T$			
Covariance matrix	$0.64\mathbf{I}_2$			
Cluster 1 size n_1	250	50	1500	100
Cluster 2 size n_2	250	50	1500	300
Cluster 3 size n_3	250	50	1500	50

Gaussians. The common hyperparameters and the different sizes used for the data clusters are summarized in Table 2.

For all these experiments, we performed 20 runs of the three clustering algorithms presented in the previous section: MS , BMS and SMS . In all the cases, we choose for all the algorithms the inner parameters (radius, cluster merging threshold and so forth) that are the most favorable in average for MS , to make the comparison as fair as possible (and even slightly biased against the proposed approach).

Figure 1 presents some results of the clustering process for set 2 with 100 iterations, and compares the obtained trajectories for MS and SMS . Note that, for MS , the directed paths to the modes can be observed, while for SMS (and also for BMS trajectories) they are much less visible. However, the high-density areas at the modes remain clear. Sub-plots (e) and (f) shows the found modes of both algorithms, while sub-plots (g) and (h) show the final clusters of the deterministic and the stochastic algorithms, respectively. In this specific example, deterministic mean-shift clustering ended with 14 clusters while stochastic mean-shift clustering provided only 9 clusters.

Overall results are displayed in Table 3. It can be seen that the stochas-

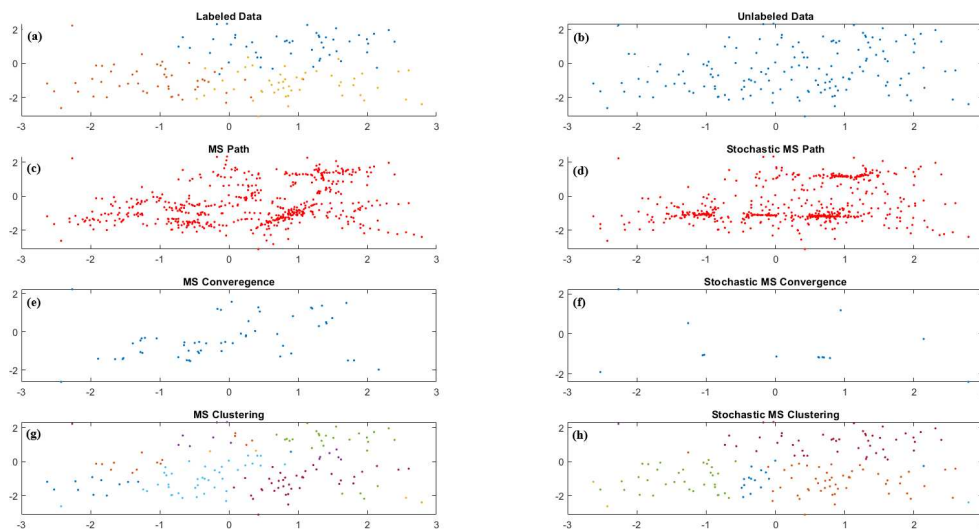


Figure 1: Results of experiment 2 (a) data with true labels; (b) unlabeled data; (c) converging paths of MS ; (d) converging paths of SMS ; (e) the found modes of MS ; (f) the found modes of SMS ; (g) the clustering of MS ; (f) the found clustering of SMS .

tic mean-shift performed better than the deterministic mean-shift in many cases, and exhibits performance comparable with BMS . In most cases, the stochastic mean-shift produced almost twice as many clusters as MS . Thus, the ALP in the stochastic case was relatively low. Indeed, the fact that points are drawn one after the other uniformly in such a case tends to leave the outlier points with little change, thus artificially increasing the number of clusters and diminishing SMS 's performance.

Set 3 has the most data points per class (1500). We notice that the number of clusters for the stochastic mean-shift is higher than for other cases. For visual inspection, we can rely on Figure 2. In that case, The data is very dense and in the deterministic case, as at the end of the convergence of one

Table 3: Average of 20 numerical criteria found on experiments 1 to 4. Best results are emphasized.

		<i>ACP</i>	<i>ALP</i>	<i>K</i>	<i>Pur(C,D)</i>	<i>Pur(D,C)</i>	<i>G</i>	Number of clusters
Set 1	MS	0.86	0.86	0.86	0.93	0.93	0.93	4.2
	BMS	0.88	0.87	0.88	0.92	0.93	0.92	3.5
	SMS	0.92	0.86	0.89	0.93	0.93	0.93	6.2
Set 2	MS	0.89	0.82	0.86	0.92	0.90	0.91	4.6
	BMS	0.89	0.86	0.88	0.91	0.92	0.92	3.7
	SMS	0.93	0.82	0.87	0.93	0.90	0.901	6.3
Set 3	MS	0.88	0.87	0.87	0.93	0.93	0.93	3.9
	BMS	0.89	0.87	0.88	0.93	0.93	0.93	3.8
	SMS	0.92	0.87	0.90	0.93	0.93	0.93	7.1
Set 4	MS	0.86	0.83	0.85	0.92	0.95	0.93	3.35
	BMS	0.88	0.84	0.86	0.95	0.95	0.95	3.9
	SMS	0.91	0.83	0.87	0.95	0.94	0.94	6.4

sample, it is placed back to the original place before starting with the next datum, all the modes are very close to each other as can be seen in subplot 2e. In contrast, in the stochastic case, no data point is placed back and at any step is updated from its current position if picked up (subplot 2f). In the deterministic case large clusters are generated during the merging along with several outliers (subplot 2g), whereas in the stochastic case we can see three well-separated clusters (subplot 2h), along with one small cluster at the intersection of the other three, the rest being outliers.

Regarding Set 4, the data is unbalanced, but the number of data points remains reasonable. From our observation, strategies updating the data's position at each iteration (whether deterministically like BMS or randomly like SMS) performed better. Indeed, updating the data positions at each iteration allows, in some sense, to escape from the attraction of large clusters, which might explain the results obtained.

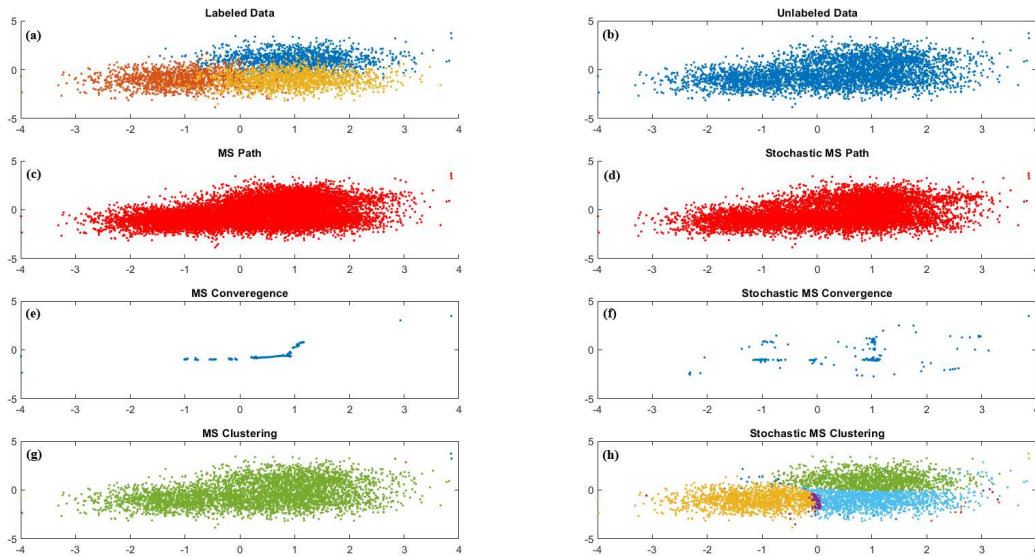


Figure 2: Results of Set 4 (a) data with true labels; (b) unlabeled data; (c) converging paths of the deterministic mean-shift; (d) converging paths of the stochastic mean-shift; (e) the modes found of the deterministic mean-shift; (f) the modes found of the stochastic mean-shift; (g) the clustering of the deterministic mean-shift; (f) the found clustering of the stochastic mean-shift.

4.3. SMS Performance Assessments

We now detail some experiments performed to evaluate several aspects of the proposed approach (each performed 100 times to get more general insight). Table 4 summarizes global information on the experiments performed.

4.3.1. Algorithmic Complexity Assessment

The first experiment compared the execution times of the three mean-shift-based clustering methods. The following experiment was repeated 100 times: given a fixed, identical number of samples per cluster, three bidimensional clusters were generated based on three 2D-Gaussian distributions.

Table 4: Hyperparameters used for the simulations

Common hyperparameters				
Maximal number of iterations	10 ⁷			
Kernel radius (bandwidth)	1			
Sample cluster distribution	$\mathcal{N}(\mu_n, \Sigma_n), \Sigma_n = 0.6\mathbf{I}_n$			
Metric	$\ x\ _2^2 = \sum_{k=1}^d x_k^2$			
Kernel type	Uniform			
Merging cluster threshold	1/3			
Convergence threshold	Change in position < 10 ⁻⁶			
	Algorithmic complexity	Influence of the class imbalance	Influence of the number of clusters	Influence of dimensionality
Number of clusters	3	3	{2...20}	3
μ_n	[1 1] ^T [-1 -1] ^T [1 -1] ^T	[1 1] ^T [-1 -1] ^T [1 -1] ^T	$\sim \mathcal{UD}(-d/2, d/2)^2$	$\sim \mathcal{UD}(\{-1, 1\})^d$
Samples per cluster	{10...10 ⁴ }	≈ 250	≈ 250	≈ 250
Samples dimension	2	2	2	{2...12}
Sample ratio per cluster	≈ 1	from 0.1 to 10	≈ 1	≈ 1

Clustering was performed using MS , BMS and SMS , and the execution times were saved. The median execution times with associated 90% confidence intervals are presented for all the methods in figure 3.

Figure 3 clearly illustrates the quadratic complexity $O(N^2)$ of both MS and BMS in contrast with the linear complexity $O(N)$ of the proposed approach. However, this claim must be tempered by the fact that, being stochastic by nature, the proposed algorithm generally requires more iterations to reach convergence than its counterparts. As a result, for problems of modest size, the deterministic approach can be more efficient, since its higher per-iteration cost is offset by faster convergence and the absence of sampling noise. However, as the sample size N increases, the quadratic growth in computational burden of the deterministic method quickly dominates. At the same time, the stochastic algorithm’s linear scaling allows it to remain computationally tractable even when many more iterations are needed. We therefore infer that SMS can become increasingly advantageous for high-dimensional

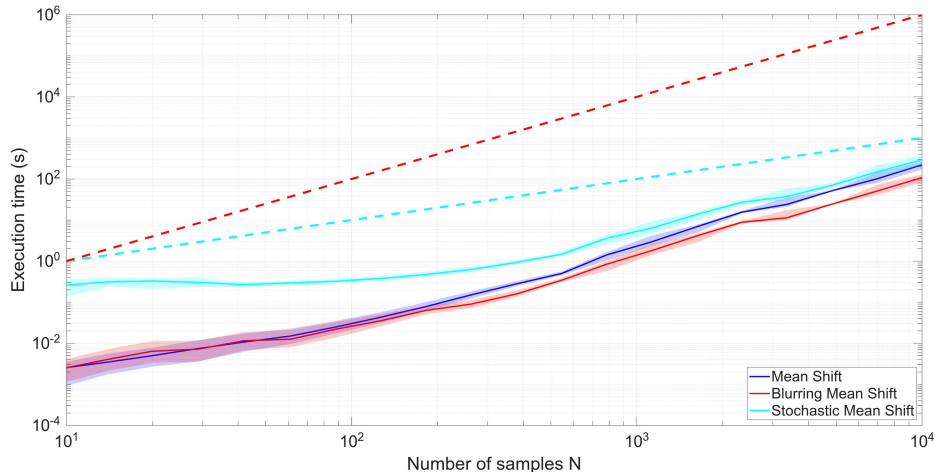


Figure 3: Execution times for MS (blue), BMS (red), and SMS (cyan), as a function of the number of points per cluster. Dotted lines illustrate linear complexity (cyan) and quadratic complexity (red) for visual comparison.

problems, where its lower asymptotic complexity compensates for its slower convergence dynamics.

4.3.2. Influence of the Cluster Imbalance

We present results for ACP and K when the proportion of points belonging to one specific cluster evolves. In this experiment, we wish to investigate how all algorithms behave when one class becomes significantly dominant with respect to the others. Median results and 90% confidence intervals are presented in Figures 4a and 4b for ACP and K, respectively.

It can be understood from figure 4a that SMS generally outperforms MS and BMS in terms of average cluster purity. Though the deterministic mean-shift seems to perform better for significant imbalance when looking at K, the observation is misleading. Indeed, when one cluster largely dominates

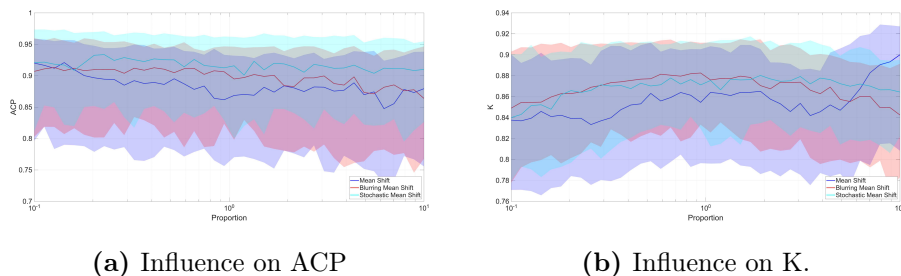


Figure 4: Influence of the class imbalance on clustering results for MS (blue), BMS (red) and SMS (cyan).

the others, the ALP tends to be one for the ordinary mean-shift, as all the data tend, in that case, to aggregate to a single cluster. This leads to an artificial increase of the K value for large disproportions between clusters, whereas BMS and SMS performance remain consistent.

4.3.3. Influence of the Data Dimensionality

Besides the number of points per cluster, their dimension also strongly influences the clustering results. For this experiment, the Gaussian averages were drawn accordingly to a discrete uniform distribution in $\{-1, 1\}^d$, where d denotes the data’s dimension. Results on ACP and K are presented in Figures 5a and 5b, respectively.

We observe that SMS outperforms MS and does slightly better than BMS when looking at the ACP criterion, whereas for the K parameter, its performance lies in between MS and BMS. All algorithms provide satisfactory results in low dimensions, whereas for higher dimensions, the SMS could be preferred for better results. As the data dimension increases and the number of labels remains constant, the clustering operation is made easier (leading to a high value of the ACP) whereas the ALP decreases drastically along with K.

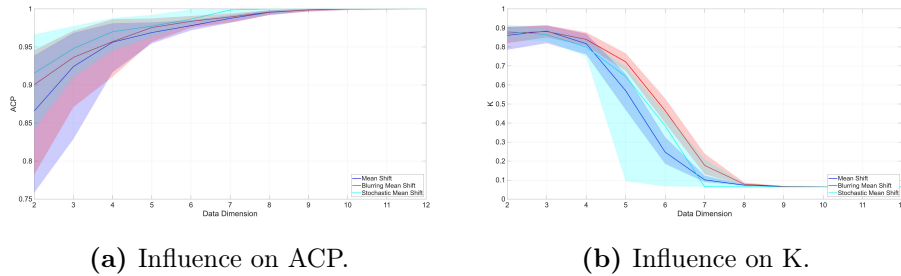


Figure 5: Influence of the data dimension on clustering results for MS (blue), BMS (red) and SMS (cyan).

4.3.4. Influence of the Number of Clusters

Eventually, we investigate how the number of classes influences the clustering process. For this experiment, the Gaussian averages were drawn accordingly to a discrete uniform distribution in $\{-R/2, R/2\}^R$, where R denotes the number of true classes. In some cases, this choice allows partial overlap between clusters, though overall the clustering task remains easy. Results on ACP and K are presented in Figures 6a and 6b, respectively.

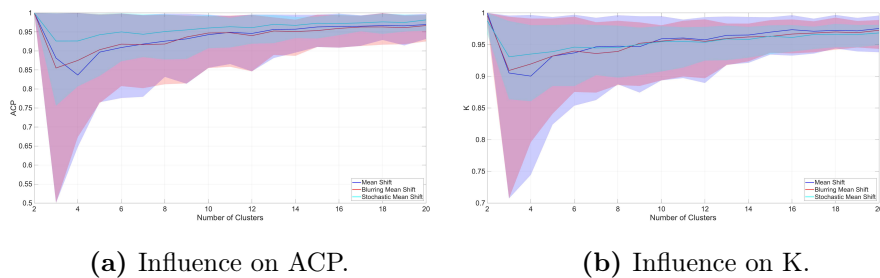


Figure 6: Influence of the number of clusters on clustering results for MS (blue), BMS (red) and SMS (cyan).

Again, we observe that SMS slightly outperforms other approaches, while the improvement becomes marginal as the number of clusters increases. We

conclude that in most cases, the proposed algorithm is on par with the state of the art BMS and often behaves better than both deterministic approaches, particularly for unbalanced classes.

5. Application to Speaker Clustering

We present in this section an application of SMS to speaker clustering. The presented results were developed in [32], and are reproduced in this paper for convenience. Among other tasks, speaker clustering appears in speaker diarization [33, 34, 35], which combines speaker segmentation as a first step and then applies a speaker clustering method. In this framework, the *ACP* and the *ALP* measures (in the original papers named *average speaker purity - ASP*) as well as the *K* value are commonly used to assess clustering validity [36, 15]. Our results involve a large number of speakers, from 3 to 60 in our simulations. The segments duration is about 2.5 s on average and the speaker segments are embedded as i-vectors.

We relied on the same database as in [13, 14, 15], based on the NIST 2008 Speaker Recognition Database [37], and used the test corpus short2-short3-Test7 for male speakers only (198 speakers in total). Mel Frequency Cepstral Coefficients (MFCC) and log energies were extracted from 25 ms frames (each one multiplied by a Hamming window), at the ratio of 19 MFCCs and one log energy extracted per 10 ms segment. For each frame, cepstral mean subtraction and variance normalization were performed on MFCCs, then delta and delta delta coefficients were calculated to finally yield a 60-dimensional features vector.

In the NIST 2008 database, the speech files consist of 5 minutes phone

speech. In the database we used, we already had i-vectors from an already segmented short speech segments. The distribution of the segment length L has minimal length of $L_{min} = 0.7$ s and average length $L_{av} = 2.5$ s. Its distribution can be approximated using an exponential distribution.

$$L \sim L_{min} + \exp(\lambda); \quad \lambda = \frac{1}{L_{av} - L_{min}}$$

The average number of segments per speaker is of $\eta = 34$ and standard deviation of $\sigma = 6.0$. This distribution of the number of speakers S can be approximated using Gaussian distribution, $S \sim \mathcal{N}(\eta, \sigma^2)$.

Following [13, 14], the Probabilistic Linear Discriminant Analysis (PLDA) scores matrix [38] was used to provide distance measures between points; at each step of both MS and SMS algorithms the neighborhood of any given point will be defined as the kNN neighborhood (with $k = 17$ in our application) w.r.t the PLDA scores related to this point.

We present the PLDA-based SMS algorithm for speaker clustering detailed in [39]. In this framework, $\mathcal{X} = \{\mathbf{x}_j\}_{j=1}^n$ is a set of normalized i-vectors. The clustering algorithm includes three steps. First, a preprocessing step is performed, which includes a principal component analysis on the ℓ_2 normalized data $\{\tilde{\mathbf{x}}_j := \mathbf{x}_j / \|\mathbf{x}_j\|\}_{j=1}^n$ to reduce data dimensionality from d to $q < d$. We apply further a whitening matrix W to the projected data on the PCA subspaces $\{T(\tilde{\mathbf{x}}_j)\}_{j=1}^n$ and renormalize:

$$\forall j \in [n] \quad \varphi_j = \frac{W T(\tilde{\mathbf{x}}_j)}{\|W T(\tilde{\mathbf{x}}_j)\|}. \quad (21)$$

Then, an integer $i \in [n]$ is drawn, and we find the subset $S_k(\varphi_i) \subseteq [n]$ containing the indices j having the k highest PLDA scores $s(\varphi_j, \varphi_i)$, and we

move the point \mathbf{x}_i to its new location:

$$\mathbf{x}_i \leftarrow \frac{\sum_{j \in S_k(\varphi_i)} \mathbf{x}_j}{\#S_k(\varphi_i)}. \quad (22)$$

More details on the algorithm can be found in [39].

The comparison between mean-shift based speaker clustering algorithms, deterministic and stochastic, in terms of *ACP*, *ALP* and *K*, is shown in Table 5. In addition, the *average number of detected speakers* (ANDS) is presented. Following [15] we compare the algorithms for 3, 7, 15, 22, 30 and 60 speakers. Each experiment was repeated 20 times with randomly chosen speakers and randomly chosen segments per speaker.

Table 5: Diarization results using MS and SMS . For each value the result is given as **mean(std)**. The last column shows the number of times that SMS achieved better performance than MS out of 20 repetitions.

Speakers	Deterministic Mean-Shift				Stochastic Mean-Shift				<i>SMS > MS</i>
	ACP	ALP	K	ANDS	ACP	ALP	K	ANDS	
3	0.99 (0.02)	0.76 (0.14)	0.86 (0.08)	6.9 (3.1)	0.97 (0.09)	0.87 (0.12)	0.91 (0.08)	7.0 (2.5)	13
7	0.93 (0.07)	0.77 (0.08)	0.85 (0.06)	13.4 (2.8)	0.92 (0.10)	0.85 (0.08)	0.88 (0.07)	16.1 (3.1)	16
15	0.92 (0.04)	0.75 (0.06)	0.83 (0.04)	26.4 (2.7)	0.89 (0.05)	0.82 (0.05)	0.86 (0.04)	29.7 (3.2)	19
22	0.86 (0.04)	0.73 (0.05)	0.79 (0.04)	36.8 (2.6)	0.83 (0.06)	0.79 (0.05)	0.81 (0.04)	41.9 (4.2)	13
30	0.82 (0.04)	0.68 (0.05)	0.75 (0.04)	46.8 (5.2)	0.78 (0.05)	0.76 (0.04)	0.77 (0.04)	51.0 (3.7)	14
60	0.75 (0.03)	0.67 (0.03)	0.71 (0.03)	78.9 (4.2)	0.68 (0.04)	0.75 (0.02)	0.71 (0.03)	86.4 (5.6)	13

Overall, SMS performs better than MS for *K*, except for the case of 60 speakers where *K* was the same. More precisely, the ALP in the stochastic case is significantly higher than in the deterministic case, whereas the ACP is slightly higher in the deterministic case. This result is surprising: typically SMS produces more clusters than MS , suggesting i-vectors from one

speaker might be split across more clusters, contrary to our findings. A possible explanation is that by isolating outliers into specific clusters, SMS steps become less sensitive to their presence, resulting in an improved clustering adequacy overall. Note that SMS was better than MS in 73.3% of the cases (88 out of 120 trials), and outperform MS independently of the number of speakers (based on the last column in Table 5).

6. Conclusion

In this work, we presented a stochastic version of the mean-shift clustering algorithm, SMS . Results illustrating its convergence were presented. We investigated the robustness of SMS in terms of number of clusters, dimensionality, computation times and class imbalance. Results showed that the proposed approach outperformed the ordinary Mean-Shift in most of the cases, and the more recent Blurring Mean-Shift in many of them. Furthermore, on the specific application of speaker clustering, we showed SMS 's potential in providing clusters of better quality than the commonly used Mean-Shift, which can be of great interest for practical applications. Further work is needed regarding the hyperparameters' optimal tuning. Moreover, this approach also raises the question of whether other hyperparameters could be drawn randomly for further improvements. These questions will be investigated in future contributions.

References

- [1] S. Lloyd, Least Squares Quantization in PCM, IEEE Transactions on Information Theory 28 (1982) 129–137. doi:10.1109/TIT.1982.1056489.

- [2] J. Shi, J. Malik, Normalized Cuts and Image Segmentation, in: Proceedings of the IEEE Conference on Computer Vision and Pattern Recognition (CVPR), 2000, pp. 731–737. doi:10.1109/CVPR.2000.854847.
- [3] A. Ng, M. Jordan, Y. Weiss, On Spectral Clustering: Analysis and an Algorithm, in: Advances in Neural Information Processing Systems (NeurIPS), volume 14, 2002, pp. 849–856.
- [4] M. Ester, H.-P. Kriegel, J. Sander, X. Xu, A Density-Based Algorithm for Discovering Clusters in Large Spatial Databases with Noise, in: Proceedings of the Second International Conference on Knowledge Discovery and Data Mining (KDD), AAAI Press, 1996, pp. 226–231.
- [5] K. Fukunaga, L. Hostetler, The Estimation of the Gradient of a Density Function, with Applications in Pattern Recognition, IEEE Transactions on Information Theory 21 (1975) 32–40. doi:10.1109/TIT.1975.1055330.
- [6] Y. Cheng, Y. Cheng, Mean Shift, Mode Seeking, and Clustering, IEEE Transactions on Pattern Analysis and Machine Intelligence 7 (1995) 790–799. doi:10.1109/34.400568.
- [7] M. A. Carreira-Perpiñán, Fast Nonparametric Clustering with Gaussian Blurring Mean-Shift, in: Proceedings of the 23rd International Conference on Machine Learning, 2006, pp. 153–160. doi:10.1145/1143844.1143864.
- [8] C. Saptarshi, P. Debolina, S. Das, Automated Clustering of High-Dimensional Data with a Feature Weighted Mean Shift Algorithm, in:

The Thirty-Fifth AAAI Conference on Artificial Intelligence (AAAI-21), 2021, pp. 6930–6939. doi:10.1609/aaai.v35i8.16854.

- [9] J. Lu, J. Chen, J. Zhang, L. Zou, Medical Image Segmentation Using Mean Shift Algorithm and General Edge Detection, in: IFAC Proceedings Volumes, volume 44, 2011, pp. 9656–9661. doi:10.3182/20110828-6-IT-1002.02861.
- [10] X. Ai, L. and Gao, J. Xiong, Application of Mean-Shift Clustering to Blood Oxygen Level Dependent Functional MRI Activation Detection, BMC Medical Imaging 14 (2014) 1–10. doi:https://doi.org/10.1186/1471-2342-14-6.
- [11] X. Wu, G. and Zhao, S. Luo, Histological Image Segmentation Using Fast Mean Shift Clustering Method, BioMed Eng OnLine 14 (2015). doi:10.1186/s12938-015-0020-x.
- [12] J. Wang, B. Thiesson, Y. Xu, M. Cohen, Image and Video Segmentation by Anisotropic Kernel Mean Shift, in: Computer Vision - ECCV 2004, 2004, pp. 238–249. doi:10.1007/978-3-540-24671-8_19.
- [13] I. Salmun, I. Opher, I. Lapidot, On the Use of PLDA i-vector Scoring for Clustering Short Segments, in: ODYSSEY 2016 Speaker and Language Recognition Workshop, 2016, pp. 407–414. doi:10.21437/Odyssey.2016-59.
- [14] I. Salmun, I. Opher, I. Lapidot, Improvements to PLDA i-vector Scoring for Short Segments Clustering, in: 2016 IEEE International Confer-

- ence on the Science of Electrical Engineering (ICSEE), 2016, pp. 1–4. doi:10.1109/ICSEE.2016.7806108.
- [15] I. Salmun, I. Shapiro, I. Opher, I. Lapidot, PLDA-Based Mean Shift Speakers’ Short Segments Clustering, *Computer Speech and Language* 45 (2017) 411 – 436. doi:10.1016/j.csl.2017.04.006.
- [16] Y. Cohen, I. Lapidot, Speaker Clustering Quality Estimation with Logistic Regression, *Computer Speech and Language* 65 (2021) 101139. doi:10.1016/j.csl.2020.101139.
- [17] T.-L. Chen, On the Convergence and Consistency of the Blurring Mean-Shift Process, *Annals of the Institute of Statistical Mathematics* 67 (2015) 157–176. doi:10.1007/s10463-013-0443-8.
- [18] R. Yamasaki, T. Tanaka, Convergence analysis of blurring mean shift, *arXiv preprint* (2024). doi:10.48550/arxiv.2402.15146.
- [19] L. Deutsch, D. Horn, The Weight-Shape Decomposition of Density Estimates: a Framework for Clustering and Image Analysis Algorithms, *Pattern Recognition* 81 (2018) 190–199. doi:10.1016/j.patcog.2018.03.034.
- [20] M. Senoussaoui, P. Kenny, T. Stafylakis, P. Dumouchel, A Study of the Cosine Distance-Based Mean Shift for Telephone Speech Diarization, *IEEE/ACM Transactions on Audio, Speech, and Language Processing* 22 (2014) 217–227. doi:10.1109/TASLP.2013.2285474.
- [21] J. Jang, H. Jiang, MeanShift++: Extremely Fast Mode-Seeking With Applications to Segmentation and Object Tracking, in: *2021 IEEE/CVF*

- Conference on Computer Vision and Pattern Recognition (CVPR), 2021, pp. 4100–4111. doi:10.1109/cvpr46437.2021.00409.
- [22] A. Kumar, S. Das, R. Mallipeddi, UEQMS: UMAP Embedded Quick Mean Shift Algorithm for High Dimensional Clustering, in: AAAI Conference on Artificial Intelligence, 2023, pp. 8386–8395. doi:10.1609/aaai.v37i7.26011.
- [23] C. Cariou, S. Le Moan, K. Chehdi, A Novel Mean-Shift Algorithm for Data Clustering, IEEE Access 10 (2022) 14575–14585. doi:10.1109/ACCESS.2022.3147951.
- [24] J. Yang, S. Rahardja, P. Franti, Mean-Shift Outlier Detection and Filtering, Pattern Recognition 115 (2021) 107874. doi:10.1016/j.patcog.2021.107874.
- [25] S. Cheng, X. Su, B. Chen, H. Chen, D. Peng, Z. Yuan, GBMOD: A Granular-Ball Mean-Shift Outlier Detector, Pattern Recognition 159 (2025) 111115. doi:10.1016/j.patcog.2024.111115.
- [26] W. Wang, M. A. Carreira-Perpinan, Manifold Blurring Mean Shift Algorithms for Manifold Denoising, in: 2010 IEEE Computer Society Conference on Computer Vision and Pattern Recognition, 2010, pp. 1759–1766. doi:10.1109/CVPR.2010.5539845.
- [27] D. Comaniciu, P. Meer, Mean shift: A robust approach toward feature space analysis, IEEE Transactions on Pattern Analysis and Machine Intelligence 24 (2002) 603–619. doi:10.1109/34.1000236.

- [28] R. Yamasaki, T. Tanaka, Convergence Analysis of Mean Shift, *IEEE Transactions on Pattern Analysis and Machine Intelligence* 46 (2023) 6688 – 6698. doi:10.1109/tpami.2024.3385920.
- [29] C. D. Manning, P. Raghavan, H. Schütze, *Introduction to Information Retrieval*, Cambridge University Press, 2008.
- [30] N. Bolshakova, F. Azuaje, Cluster Validation Techniques for Genome Expression Data, *Signal Processing* 83 (2003) 825 – 833. doi:10.1016/S0165-1684(02)00475-9.
- [31] R. Tibshirani, G. Walther, T. Hastie, Estimating the number of clusters in a data set via the gap statistic, *Journal of the Royal Statistical Society: Series B (Statistical Methodology)* 63 (2001) 411–423. doi:10.1111/1467-9868.00293.
- [32] I. Lapidot, Stochastic mean-shift for speaker clustering, in: *2023 57th Annual Conference on Information Sciences and Systems (CISS)*, 2023, pp. 1–5. doi:10.1109/CISS56502.2023.10089776.
- [33] H. Aronowitz, W. Zhu, M. Suzuki, G. Kurata, R. Hoory, New Advances in Speaker Diarization, in: *Interspeech 2020*, 2020, pp. 279–283. doi:10.21437/Interspeech.2020-1879.
- [34] A. Silnova, N. Brummer, J. Rohdin, T. Stafylakis, L. Burget, Probabilistic Embeddings for Speaker Diarization, in: *Proc. Odyssey 2020 Speaker and Language Recognition Workshop*, 2020, pp. 24–31. doi:10.21437/Odyssey.2020-4.

- [35] Q. Lin, W. Cai, L. Yang, J. Wang, J. Zhang, M. Li, DIHARD II is Still Hard: Experimental Results and Discussions from the DKU-LENOVO Team, in: Proc. Odyssey 2020 Speaker and Language Recognition Workshop, 2020, pp. 102–109. doi:10.21437/Odyssey.2020-15.
- [36] J. Ajmera, H. Bourlard, I. Lapidot, I. McCowan, Unknown-Multiple Speaker Clustering Using HMM, in: Proceedings of ICSLP-2002, 2002, pp. 573–576. doi:10.21437/ICSLP.2002-195.
- [37] L. D. Consortium, Ldc2011s05, ldc2011s07 and ldc2011s08 catalogs, <https://catalog.ldc.upenn.edu/>, 2011.
- [38] N. Dehak, P. J. Kenny, R. Dehak, P. Dumouchel, P. Ouellet, Front-End Factor Analysis for Speaker Verification, IEEE Transactions on Audio, Speech, and Language Processing 19 (2011) 788–798. doi:10.1109/TASL.2010.2064307.
- [39] I. Lapidot, Stochastic Mean-Shift for Speaker Clustering, in: 2023 57th Annual Conference on Information Sciences and Systems (CISS), 2023, pp. 1–5. doi:10.1109/CISS56502.2023.10089776.

Stochastic mean-shift clustering - Supplementary Material

Itshak Lapidot^{a,b}, Yann Sepulcre^c, Tom Trigano^d

^a*Afeka Tel-Aviv Academic College of Engineering, School of Electrical Engineering, Israel*

^b*Avignon University, LIA, France*

^c*Sapir Academic College, Department of Engineering, Sderot, Israel*

^d*Shamoon College of Engineering, Department of Electrical Engineering, Ashdod, Israel*

Abstract

The document presents the proof of the paper “Stochastic Mean-Shift Clustering”.

Proof of Proposition 1

For any given $k \in \mathbb{N}$, we shall denote for simplicity $\mathcal{X} = \mathcal{X}^{(k)} = [\mathbf{x}_1^T, \dots, \mathbf{x}_n^T]^T$ and $\widehat{\mathcal{X}} = \mathcal{X}^{(k+1)} = [\widehat{\mathbf{x}}_1^T, \dots, \widehat{\mathbf{x}}_n^T]^T$; introducing further $i = i_k$ as the index picked up randomly at step k , we have $\forall j \in [n] \setminus \{i\} \widehat{\mathbf{x}}_j = \mathbf{x}_j$ so that

$$L(\widehat{\mathcal{X}}) - L(\mathcal{X}) = k(0) + \sum_{j \neq i} k \left(\frac{\|\widehat{\mathbf{x}}_i - \mathbf{x}_j\|^2}{h^2} \right) - \sum_j k \left(\frac{\|\mathbf{x}_i - \mathbf{x}_j\|^2}{h^2} \right) \quad (1)$$

Email addresses: itshakl@afeka.ac.il (Itshak Lapidot),
yanns@mail.sapir.ac.il (Yann Sepulcre), thomast@sce.ac.il (Tom Trigano)

In (1) the sum in the last term is on every $j \in N_h(i)$; since k has only non-negative values one can pursue as follows:

$$\begin{aligned}
L(\widehat{\mathcal{X}}) - L(\mathcal{X}) &\geq \sum_{\substack{j \in N_h(i) \\ j \neq i}} k \left(\frac{\|\widehat{\mathbf{x}}_i - \mathbf{x}_j\|^2}{h^2} \right) - k \left(\frac{\|\mathbf{x}_i - \mathbf{x}_j\|^2}{h^2} \right) \\
&\geq \frac{1}{h^2} \sum_{\substack{j \in N_h(i) \\ j \neq i}} G \left(\frac{\mathbf{x}_i - \mathbf{x}_j}{h} \right) (\|\mathbf{x}_i - \mathbf{x}_j\|^2 - \|\widehat{\mathbf{x}}_i - \mathbf{x}_j\|^2) \quad (2) \\
&= \frac{1}{h^2} \left[G(\mathbf{0}) \|\widehat{\mathbf{x}}_i - \mathbf{x}_i\|^2 + \sum_{j \in N_h(i)} G \left(\frac{\mathbf{x}_i - \mathbf{x}_j}{h} \right) (\|\mathbf{x}_i - \mathbf{x}_j\|^2 - \|\widehat{\mathbf{x}}_i - \mathbf{x}_j\|^2) \right]
\end{aligned}$$

In (2) the inequality follows from the convexity assumption on k : indeed for every $(\mathbf{u}, \mathbf{v}) \in (\mathbb{R}^n)^2$ we have $k(\|\mathbf{v}\|^2) - k(\|\mathbf{u}\|^2) \geq k'(\|\mathbf{u}\|^2) (\|\mathbf{v}\|^2 - \|\mathbf{u}\|^2) = G(\mathbf{u}) (\|\mathbf{u}\|^2 - \|\mathbf{v}\|^2)$. In the last expression above, by the very definition of

$\widehat{\mathbf{x}}_i$ as a mean point: $\widehat{\mathbf{x}}_i = \sum_{j \in N_h(i)} \frac{G \left(\frac{\mathbf{x}_i - \mathbf{x}_j}{h} \right)}{\sum_{m \in N_h(i)} G \left(\frac{\mathbf{x}_i - \mathbf{x}_m}{h} \right)} \mathbf{x}_j$, we have the simple

equality

$$\sum_{j \in N_h(i)} G \left(\frac{\mathbf{x}_i - \mathbf{x}_j}{h} \right) (\|\mathbf{x}_i - \mathbf{x}_j\|^2 - \|\widehat{\mathbf{x}}_i - \mathbf{x}_j\|^2) = \left(\sum_{j \in N_h(i)} G \left(\frac{\mathbf{x}_i - \mathbf{x}_j}{h} \right) \right) \|\mathbf{x}_i - \widehat{\mathbf{x}}_i\|^2 ;$$

it follows immediately by the non-negativity of G that

$$L(\widehat{\mathcal{X}}) - L(\mathcal{X}) \geq \frac{2G(\mathbf{0})}{h^2} \|\widehat{\mathbf{x}}_i - \mathbf{x}_i\|^2 \quad (3)$$

In turn (3) implies that $(L(\mathcal{X}^{(k)}))_{k \in \mathbb{N}}$ is a non decreasing, hence convergent sequence since it is upper bounded by the constant $\frac{n(n+1)}{2} k(0)$. As for the second

claim, it follows easily from the equality $\nabla_i L(\mathcal{X}^{(k)}) = \frac{2 \sum_{j=1}^n G \left(\frac{\mathbf{x}_i^{(k)} - \mathbf{x}_j^{(k)}}{h} \right)}{h^2} [\mathcal{X}^{(k+1)} - \mathcal{X}^{(k)}]$

hence

$$\|\nabla_i L(\mathcal{X}^{(k)})\| \leq \frac{2n|k'(0)|}{h^2} \|\widehat{\mathbf{x}}_i - \mathbf{x}_i\| \quad (4)$$

since by assumption $G(\mathbf{u}) = |k'(\|\mathbf{u}\|^2)|$ is a non increasing function of the norm $\|\mathbf{u}\|$. Now (3)(4) lead immediately to the following

$$\|\nabla_i L(\mathcal{X}^{(k)})\| \leq \frac{n\sqrt{2|k'(0)|}}{h} \left(L(\widehat{\mathcal{X}}) - L(\mathcal{X})\right)^{1/2} \quad (5)$$

which completes the proof.

Proof of Lemma 1

It is clear that $\Omega_{p+1} = \bigcup_{k=k_0+p+1}^{\infty} (T_{p+1} = k)$. The probability $\mathbb{P}(\Omega_{p+1})$ can be decomposed as follows

$$\begin{aligned} \mathbb{P}(\Omega_{p+1}) &= \sum_{k=k_0+p+1}^{\infty} \sum_{m=k_0+p}^{k-1} \mathbb{P}(T_{p+1} = k \wedge T_p = m) \\ &= \sum_{k=k_0+p+1}^{\infty} \sum_{m=k_0+p}^{k-1} \mathbb{P}(\|\nabla^{(k)}\| \geq \epsilon \wedge \|\nabla_{i_k}^{(k)}\| < \epsilon \dots \\ &\quad \wedge \forall j \in (m, \dots, k) \|\nabla^{(j)}\| < \epsilon \wedge T_p = m) \quad (6) \end{aligned}$$

Consider any given pair of integers (k, m) such that $k \geq k_0 + p + 1$ and $k_0 + p \leq m \leq k - 1$, and define the following event as a subset in $[n]^{k-1}$:

$$B_{k,m} = \{[i_{k-1}, \dots, i_0] \mid \|\nabla^{(k)}\| \geq \epsilon \wedge \forall j \in (m, \dots, k) \|\nabla^{(j)}\| < \epsilon \wedge T_p = m\} \quad (7)$$

As was mentioned previously right after (11): at any step k of SMS the state $\mathcal{X}^{(k)}$ depends solely on the random sequence of indices $[i_{k-1}, \dots, i_0]$; hence there exists a (non random) function $\mathcal{E}^{(k)} : [n]^k \rightarrow 2^{[n]}$ such that

$\{i \in [n] \mid \|\nabla_i^{(k)}\| < \epsilon\} = \mathcal{E}^{(k)} [i_{k-1}, \dots, i_0]$. As a consequence, using the assumption that the index i_k is independent of $[i_{k-1}, \dots, i_0]$ it holds that

$$\begin{aligned} \mathbb{P} \left(\|\nabla_{i_k}^{(k)}\| < \epsilon \wedge B_{k,m} \right) &= \sum_{[i_{k-1}, \dots, i_0] \in B_{k,m}} \mathbb{P} (i_k \in \mathcal{E}^{(k)} [i_{k-1}, \dots, i_0]) \mathbb{P} ([i_{k-1}, \dots, i_0]) \\ &\leq \frac{n-1}{n} \mathbb{P} (B_{k,m}) \quad ; \end{aligned} \quad (8)$$

last inequality (8) is satisfied since for all $[i_{k-1}, \dots, i_0] \in B_{k,m}$ it holds that $\|\nabla^{(k)}\| \geq \epsilon$ hence $\exists i \|\nabla_i^{(k)}\| \geq \epsilon$, implying the rough upper bound on the cardinality $\#\mathcal{E}^{(k)} [i_{k-1}, \dots, i_0] \leq n-1$. Now going back to (6) one can write:

$$\begin{aligned} \mathbb{P} (\Omega_{p+1}) &\leq \frac{n-1}{n} \sum_{m=k_0+p}^{\infty} \sum_{k=m+1}^{\infty} \mathbb{P} (B_{k,m}) \\ &\leq \frac{n-1}{n} \sum_{m=k_0+p}^{\infty} \mathbb{P} (T_p = m) = \left(1 - \frac{1}{n}\right) \mathbb{P} (\Omega_p) \quad ; \end{aligned} \quad (9)$$

indeed last inequality (9) follows from the immediate $\sum_{k=m+1}^{\infty} \mathbb{P} (B_{k,m}) \leq \mathbb{P} (T_p = m)$ which holds for any $m \in \mathbb{N}$.

Proof of Proposition 2

Given any $\epsilon > 0$, by proposition 1 for any $\omega = [i_k]_{k \in \mathbb{N}}$ and $\epsilon > 0$ it holds a.s that $\exists K(\omega) \in \mathbb{N} \forall k > K(\omega) \|\nabla_{i_k}^{(k)}\| < \epsilon$. For any $k_0 \in \mathbb{N}$ let us define the event $\mathcal{U}_{k_0} = \{K(\omega) = k_0\}$; lemma 1 shows that for the sequence of stopping times (T_p) defined with the pair (ϵ, k_0) by (14) (15) it holds that $\lim_{p \rightarrow \infty} \mathbb{P} (T_p < \infty \wedge \mathcal{U}_{k_0}) = 0$, in other words $\mathbb{P} ((\forall p \in \mathbb{N} T_p < \infty) \wedge \mathcal{U}_{k_0}) = 0$. Since $\mathbb{P} \left(\bigcup_{k_0 \in \mathbb{N}} \mathcal{U}_{k_0} \right) = 1$ by proposition 1, it follows immediately that $\mathbb{P} ((\forall p \in \mathbb{N} T_p < \infty)) = 0$, in other words there is a.s. on ω an integer $K_1(\omega)$ such that $\forall k \geq K_1(\omega) \|\nabla^{(k)}(\omega)\| < \epsilon$. The result is proved.

Proof of Theorem 2

Consider the following event \mathcal{B} (in the condition below (k_p) denotes an infinite integers sequence):

$$\mathcal{B} = \left\{ \omega \mid \exists (k_p) \quad \forall p \in \mathbb{N} \exists (i, j) \in [n]^2 \quad \tau \leq \|\mathbf{x}_i^{(k_p)} - \mathbf{x}_j^{(k_p)}\| \leq h - \tau \right\}$$

For any $\omega \in \mathcal{B}$, considering a subsequence of states $[\mathcal{X}^{(k_p)}]$ satisfying the condition above, clearly there exist two distinct and fixed integers $i \neq j$ in $[n]$ such that for an infinity of integers (k_{p_m}) one has $\tau \leq \|\mathbf{x}_i^{(k_{p_m})} - \mathbf{x}_j^{(k_{p_m})}\| \leq h - \tau$ for any $m \in \mathbb{N}$. By compactness one can further extract some subsequence of $[\mathcal{X}^{k_{p_m}}]$ which tends to some $\bar{\mathcal{X}} \in \mathbb{R}^{dn}$ (indeed, for any $k \in \mathbb{N}$ all the points $\mathbf{x}_i^{(k)}$ belong to the convex envelop $\text{conv}(\mathbf{x}_i^{(0)}, i \in [n])$ which is compact); but it would imply that $\tau \leq \|\bar{\mathbf{x}}_i - \bar{\mathbf{x}}_j\| \leq h - \tau$, hence $\nabla L(\bar{\mathcal{X}}) \neq \mathbf{0}$ by theorem 1. By our assumption L is C^1 , so the previous argument shows the inclusion $\mathcal{B} \subseteq \{\omega \mid \nabla^{(k)} \not\rightarrow \mathbf{0}_{dn}\}$, and since the latter subset is of measure 0 by proposition 2 it follows that $\mathbb{P}(\mathcal{B}) = 0$.

Therefore, it holds almost surely on ω that there exists $K = K(\omega) \in \mathbb{N}$ such that the following two conditions hold

$$\forall k \geq K \quad \forall (i, j) \in [n]^2 \quad \|\mathbf{x}_i^{(k)} - \mathbf{x}_j^{(k)}\| < \tau \quad \vee \quad \|\mathbf{x}_i^{(k)} - \mathbf{x}_j^{(k)}\| > h - \tau \quad (10)$$

$$\forall k \geq K \quad \|\nabla^{(k)}\| \leq \frac{2G(\mathbf{0})}{h^2} (h - 2\tau); \quad (11)$$

suppose now that two integers $(i, j) \in [n]^2$ satisfies for some $k \geq K$ that $\|\mathbf{x}_i^{(k)} - \mathbf{x}_j^{(k)}\| < \tau$ and $\|\mathbf{x}_i^{(k+1)} - \mathbf{x}_j^{(k+1)}\| > h - \tau$ (or these two inequalities in opposite order, the argument will stay the same); since at any step

SMS modifies one point only, we may assume that $\mathbf{x}_j^{(k+1)} = \mathbf{x}_j^{(k)}$ and therefore

$$\begin{aligned} \|\mathbf{x}_i^{(k+1)} - \mathbf{x}_i^{(k)}\| &\geq \|\mathbf{x}_i^{(k+1)} - \mathbf{x}_j^{(k+1)}\| - \|\mathbf{x}_i^{(k)} - \mathbf{x}_j^{(k)}\| \\ &> h - 2\tau \end{aligned} \tag{12}$$

which contradicts this other property which follows directly from (11) and assumption (11) above: $\|\mathbf{x}_i^{(k+1)} - \mathbf{x}_i^{(k)}\| \leq \frac{h^2}{2G(\mathbf{0})} \|\nabla^{(k)}\| \leq h - 2\tau$. In other words conditions (10)(11) above imply the existence of some (fixed) partition J_1, \dots, J_M of $[n]$ satisfying for every $k \geq K$ conditions 1)2) in the theorem. Since τ was arbitrary positive the diameter of each cluster \mathcal{C}_l , $l \in [M]$ tends a.s to 0 as $k \rightarrow \infty$.

Proof of Theorem 3

For any finite set $S \subset \mathbb{R}^d$ of points, we shall denote by $\text{conv}(S)$ the convex hull of S which in this case is a compact set; since for any $k \in \mathbb{N}$ we have $\text{conv}(\mathcal{X}^{(k+1)}) \subseteq \text{conv}(\mathcal{X}^{(k)})$, it follows that $\exists \mathbf{z} \in \bigcap_{k \in \mathbb{N}} \text{conv}(\mathcal{X}^{(k)})$; by defining the transformed state $\widehat{\mathcal{X}}^{(0)} = [(\mathbf{x}_1^{(0)} - \mathbf{z})^T, \dots, (\mathbf{x}_n^{(0)} - \mathbf{z})^T]^T$ we shall consider from now that $\mathbf{z} = \mathbf{0}_d$, with the algorithm proceeding as usual with $\widehat{\mathcal{X}}^{(0)}$ as the original state. In this case we shall prove that for any $i \in [n]$:

$$\lim_{k \rightarrow \infty} \mathbf{x}_i^{(k)} = \mathbf{0}_d.$$

Let $\mathbf{u} \in \mathbb{R}^d$ be any unit vector, and denote by $\pi_{\mathbf{u}} : \mathbb{R}^d \rightarrow L_{\mathbf{u}}$ the orthogonal projection operator on the line $L_{\mathbf{u}} = \mathbb{R}\mathbf{u}$. For any $k \in \mathbb{N}$ we define the projected points $y_i^{(k)} = \pi_{\mathbf{u}}(\mathbf{x}_i^{(k)})$ on $L_{\mathbf{u}}$ for any $i \in [n]$, and consider these as n real numbers. By the linearity of $\pi_{\mathbf{u}}$ the sequence of states

$\left(\left[y_1^{(k)}, \dots, y_n^{(k)}\right]\right)_{k \in \mathbb{N}}$ (here a state is a point in \mathbb{R}^n) is updated by the rule:

$$i = i_k : y_i^{(k+1)} = \frac{\sum_{j \in [n]} G\left(\frac{\mathbf{x}_i^{(k)} - \mathbf{x}_j^{(k)}}{h}\right) y_j^{(k)}}{\sum_{j \in [n]} G\left(\frac{\mathbf{x}_i^{(k)} - \mathbf{x}_j^{(k)}}{h}\right)} ; \quad (13)$$

note that the summations above are on all $j \in [n]$ since $N_h(i) = [n]$. For any $k \in \mathbb{N}$ define $m^{(k)} = \min\{y_i^{(k)}, i \in [n]\}$, $M^{(k)} = \max\{y_i^{(k)}, i \in [n]\}$; the sequence $(m^{(k)})$ (resp. $(M^{(k)})$) is non decreasing (resp. non increasing), hence both sequences converge to real numbers: $\lim_{k \rightarrow \infty} m^{(k)} = m \leq M = \lim_{k \rightarrow \infty} M^{(k)}$. We now show that $m = M$ holds a.s, or in other words that $\mathbb{P}(\{m < M\}) = 0$. Suppose ω satisfies $m(\omega) < M(\omega)$, and let $\epsilon > 0$ be any positive value which shall be chosen conveniently below; so there exists an integer K_0 such that for all $k \geq K_0$ we have $m - \epsilon < m^{(k)}$. Given any such $k \geq K_0$, denote by i_k the chosen integer, and let $j_k \in [n]$ be some integer such that $y_{j_k}^{(k)} \geq M$ (there has to be one at least); we denote also the positive weights in (13) simply as follows: $\forall p \in [n] w_p := G\left(\frac{\mathbf{x}_{i_k}^{(k)} - \mathbf{x}_p^{(k)}}{h}\right)$. It holds that

$$\forall k \geq K_0 \quad y_{i_k}^{(k+1)} > \frac{\sum_{p \neq j_k} w_p (m - \epsilon) + w_{j_k} M}{\sum_{p \neq j_k} w_p + w_{j_k}} ;$$

now for ϵ chosen sufficiently small the quantity on the RHS of the previous inequality is greater than m , as this property is equivalent to $w_{j_k} (M - m) > (\sum_{p \neq j_k} w_p) \epsilon$ which is guaranteed if we choose $\epsilon < \frac{|k' \left(\frac{\text{diam}(\mathcal{X}^{(0)})^2}{h^2}\right)|}{(n-1)|k'(0)|} (M - m)$, since $\text{diam}(\mathcal{X}^{(k)})$ is a decreasing sequence. So far we have proved that for any ω such that $m(\omega) < M(\omega)$ there is a K_0 (depending on ω) such that

$\forall k \geq K_0$ $y_{i_k}^{(k+1)} > m$; since the indices $i_k \sim \mathcal{U}_{[n]}$ are i.i.d every $i \in [n]$ will be picked at least once within a finite number of steps after K_0 a.s., such event implying that $\exists K_1$ $m^{(K_1)} > m$, a contradiction by the monotonicity of $m^{(k)}$. Since $K_0 \in \mathbb{N}$, the event $\{m < M\}$ is expressed as a denumerable union of null measure subsets, hence $\mathbb{P}(\{m < M\}) = 0$ as claimed.

By assumption $\forall k \in \mathbb{N}$ $0 \in \text{conv}(y_i^{(k)}, i \in [n]) = [m^{(k)}, M^{(k)}]$, so the fact that $\lim_{k \rightarrow \infty} M^{(k)} - m^{(k)} = 0$ holds a.s. implies that for all $\mathbf{u} \in \mathbb{R}^d$ and for each $i \in [n]$ one has $\lim_{k \rightarrow \infty} \pi_{\mathbf{u}}(\mathbf{x}_i^{(k)}) = 0$ a.s. The same argument can be used for any unit vector $\mathbf{u} \in \mathbb{R}^d$, so the theorem is proved.